The Cryosphere Discuss., https://doi.org/10.5194/tc-2019-17
Manuscript under review for journal The Cryosphere
Discussion started: 5 March 2019

Very old firn air linked to strong density layering at Styx Glacier, coastal Victoria Land, East Antarctica

Youngjoon Jang[1], Sang Bum Hong[2], Christo Buizert[3], Hun-Gyu Lee[1], Sang-young Han[1], Ji-Woong Yang[1], Yoshinori Iizuka[4], Akira Hori[5], Yeongcheol Han[2], Seong Joon Jun[2], Pieter Tans[6], Taejin Choi[2], Seong-Joong Kim[2], Soon Do Hur[2], and Jinho Ahn[1*]

[1]School of Earth and Environmental Sciences, Seoul National University, Seoul, Republic of Korea

[2]Korea Polar Research Institute, Incheon, Republic of Korea

[3]College of Earth, Ocean, and Atmospheric Sciences, Oregon State University, Corvallis, Oregon, USA

[4]Institute of Low Temperature Science, Hokkaido University, Sapporo, Japan

[5]Kitami Institute of Technology, Kitami, Japan

[6]National Oceanic and Atmospheric Administration, Earth System Research Laboratory, Boulder, CO, USA

Corresponding to: Jinho Ahn (jinhoahn@gmail.com)

Abstract

Firn air provides plenty of old air from the near past, and can therefore be useful for understanding human impact on the recent history of the atmospheric composition. Most of the existing firn air records cover only the last several decades (typically 40 to 55 years) and are insufficient to understand the early part of anthropogenic impacts on atmosphere. In contrast, a few firn air records from inland sites, where temperatures and snow accumulation rates are very low, go back in time about a century. In this study, we report an unusually old firn air age of 89 years from Styx Glacier, near the Ross Sea coast in Antarctica. This is the first report of such an old firn air age (> 55 years) from a warm coastal site. The lock-in zone thickness of 12.4 m is larger than at other sites where snow accumulation rates and air temperature are similar. High-resolution X-ray density measurements demonstrate a high variability of the vertical snow density at Styx Glacier. The CH_4 mole fraction and total air content of the closed pores also indicate large variations in cm-scale depth intervals, indicative of layering. We hypothesize that the large density variations in the firn increase the thickness of lock-in zone and

The Cryosphere Discuss., https://doi.org/10.5194/tc-2019-17
Manuscript under review for journal The Cryosphere
Discussion started: 5 March 2019

The Cryosphere
Discussions
Open Access

consequently increase firn air ages because the age of firn air rapidly increase with depth in the lock-in zone. Our study demonstrates that sites where weather conditions are favorable for the formation of large density variations at the lock-in zone preserve very old air within their open porosity, making them ideal places for firn air sampling.

1 Introduction

Bubbles trapped in ice cores preserve ancient air and allow direct measurements of the atmospheric composition in the past (e.g., Petit et al., 1999). However, it is difficult to obtain air samples over the past several decades from those ice cores since the more recent air has not yet been completely captured into bubbles closed off from the atmosphere. In contrast, we can obtain the recent records from the interstitial air in the porous, unconsolidated snow layer (firn) on top of glaciers and ice sheets (Etheridge et al., 1996, 1998). In addition, we can take advantage of the very large amount of firn air because it allows us to accurately analyze isotopic ratios of greenhouse gases and many trace gases such as man-made CFCs, HCFCs and SF_6 (Buizert et al., 2012a; Laube et al., 2012). However, reported firn air ages date back only several decades at the sites where snow accumulation rates are relatively high (Table 1). Old firn air (> 55 years) was observed only at sites where surface temperatures and snow accumulation rates are low such as South Pole and inland Antarctic Megadunes (Table 1); however, even under such circumstances very old firn air is not guaranteed, as demonstrated by Dome C (Table 1).

In the firn layer, air moves through the open pores and is occluded into the adjacent ice at the typical close-off density (Schwander, 1989). The firn air moves downward with the adjacent ice (advection), but is furthermore mixed by diffusion, and affected by thermal and gravitational fractionation (Craig et al., 1988; Johnsen et al., 2000; Severinghaus et al., 2001; Goujon et al., 2003). In addition, the gradual bubble trapping in the firn affects the movement of the air. As a result, at each depth there is a gas age distribution (Trudinger et al., 1997), rather than a single gas age. Therefore, studying firn air is also important for interpreting the record of ancient air trapped in ice cores.

The firn column is generally divided into three zones; convective, diffusive and lock-in zones, depending on the mechanisms of firn air movement (Sowers et al., 1992). The convective zone is the upper part of the firn

The Cryosphere Discuss., https://doi.org/10.5194/tc-2019-17
Manuscript under review for journal The Cryosphere
Discussion started: 5 March 2019

where the air can ventilate with the overlying atmosphere. With stronger wind pumping, there can be a deeper convective zone (Kawamura et al., 2013). This zone has the same $\delta^{15}N$ of N_2 value as that of the atmosphere. The diffusive zone is located under the convective zone, where molecular diffusion of the firn air dominates transport mechanism of the firn air (Blunier and Schwander, 2000). The age of the firn air increases slowly with depth in the diffusive zone because of continued gas exchange with atmospheric air via diffusion. Heavier isotopes are enriched with depth due to the gravitational fractionation in the stagnant diffusive layer. Thus, $\delta^{15}N$ of N_2 gradually increases with depth in the diffusive zone. In the lock-in zone (LIZ) below the diffusive zone, gas diffusion is strongly impeded although the bubbles are not entirely closed. The top of the lock-in zone is called lock-in depth (LID), where the gravitational fractionation ceases, so that the $\delta^{15}N$ of N_2 becomes constant. The bottom of the LIZ is defined as the close-off depth (COD), where all air bubbles are closed off and firn becomes mature ice. The COD can be estimated in two different ways. First, we can calculate the COD from firn densification models. Typically, the close-off occurs the density of ice reaches about 830 kg m^{-3} (Blunier and Schwander, 2000). – equivalent to a critical porosity of around 0.1 (Schaller et al., 2017). Also, if temperature is known, the average density at close-off can be estimated from empirical relations (Martinerie et al., 1992). Second, the deepest position where air can be sampled from the firn column is commonly considered as (just above) the COD. In theory, the COD is the depth at which all pores are closed, but it can be ambiguous to specify the COD in the field because firn air can be sampled at a slightly deeper depth than that of the shallowest impermeable snow layer due to the existence of permeable layers at deeper depths – this effect is due to density layering (Mitchell et al., 2015).

The gas ages in the LIZ increase with depth faster than in the diffusive zone. In the LIZ, firn air moves downward at (nearly) the same rate as the surrounding ice, and therefore the age of the air increases with depth at the same rate as the age of ice.

The age of the firn air is directly related to the movement of the firn air. We define the oldest firn air age as the mean age at the deepest sampling depth. The firn air models help calculate the firn air age using some parameters such as temperature and accumulation rate. However, several studies found that the layering also affects the movement of the firn air (e.g., Mitchell et al., 2015; Schaller et al., 2017). This implies that physical properties of the ice may affect the age of the firn air as well.

The Cryosphere Discuss., https://doi.org/10.5194/tc-2019-17
Manuscript under review for journal The Cryosphere
Discussion started: 5 March 2019

The Cryosphere Discussions

With regard to the lock-in and close-off processes, recent studies have focused on snow layers and microstructure of the firn (Hörhold et al., 2011; Gregory et al., 2014; Mitchell et al., 2015; Schaller et al., 2017). Density variability on millimeter to tens of cm scales is observed in all polar sites. Hörhold et al. (2011) demonstrate that density variability is caused by physical snow properties in the firn column. Several studies have dealt with how snow density variations affect the transport of firn air (Hörhold et al., 2011; Mitchell et al., 2015). Mitchell et al. (2015) showed that the firn layering can affect the closure of pores and the thickness of LIZ, but the relation between snow density variations and range of firn air ages was not quantitatively examined.

In this study, we present firn air compositions and $\delta^{15}N$-N_2 from Styx Glacier, East Antarctica to better understand the role of snow density variations on the age of firn air. We also present X-ray density data with millimeter resolutions and compare them with $\delta^{18}O_{ice}$ and the closed-pore air compositions in the LIZ.

We hypothesize that large snow density variations make the LIZ thicker and facilitate preservation of old firn air at the Styx Glacier. This study will help us better understand how the snow density layers of firn column affects movement and preservation of firn air, and provide guidance on selecting good sites for future firn air studies.

2 Materials and Methods

2.1 Firn air sampling and gas mole fractions analysis

The firn air and ice core were sampled at the Styx Glacier, East Antarctica (73° 51.10' S, 163° 41.22' E, 1623 m asl) in December of 2014 (Fig. 1). This site is located 85 km north of the Korean Jang Bogo Station in the Southern Cross Mountains near the Ross Sea (Han et al., 2015). The snow accumulation rate is ~10 cm ice year^{-1} that calculated from the Styx16b ice chronology based on methane correlation and tephra age tie-point and thinning functions (Yang et al., 2018). The mean annual surface temperature was measured as -31.7℃ by borehole temperature logging at 15 m depth, two year after the ice core drilling (Yang et al., 2018). Table 1 lists the characteristics of the Styx Glacier and other firn air sampling sites. A total of 13 samples from the surface to 64.8 m depth were collected. The firn air sampling device was constructed, following the design of that of the University of Bern, Switzerland (Schwander et al., 1993). Three vacuum pumps (two diaphragm pumps and one metal bellows pump), several pressure gauges, stainless steel lines, and vacuum valves were housed in an

The Cryosphere Discuss., https://doi.org/10.5194/tc-2019-17
Manuscript under review for journal The Cryosphere
Discussion started: 5 March 2019

aluminum case to transfer to the polar site. The pump system plays four major roles: (1) purging modern air from the bottom of a borehole, (2) inflating the bladder to block the deep firn layers from the atmosphere, (3) removing the contaminated air and extracting the firn air, (4) transporting firn air to a CO_2 analyzer for measurements of gas mole fractions and store it in firn air containers. The bladder system is designed to be lowered into the borehole to seal the deep firn layer(s) being sampled from the atmosphere. The bladder consists of a 4 m-long rubber tube and metal caps on top and bottom of the rubber tube. The bladder's external diameter is 119.5 mm and internal diameter is 114.5 mm. The material of the tube is butyl rubber (BIIR) which can endure being inflated in low temperatures.

The firn air samples were collected in 3-liter glass flasks at all collection depths. However, to test preservation ability of the sample air containers, Silcocan canisters were also used at 4 depths (0, 35.36, 43.42, 53.95 m). Accurate mole fractions of CO_2, CH_4, and SF_6 were measured at US National Oceanic and Atmospheric Administration (NOAA; https://www.esrl.noaa.gov/). The results for the two types of containers show good agreements. $\delta^{15}N$ of N_2 was analyzed at Scripps Institution of Oceanography for correcting gravitational fractionation effect (Severinghaus et al., 2010).

2.2 Firn air transport model

We used the Center for Ice and Climate (CIC) firn air model which is a 1-dimensional diffusion model to simulate how the air moves in Styx firn column. In this model, there are 4 types of transport in the open porosity: (1) molecular diffusion, (2) vigorous mixing in the convective zone, (3) advection, and (4) dispersion in the deep firn (Buizert, 2012b, Buizert and Severinghaus, 2016). A velocity of the air is represented as w_{air} in open pores.

$$w_{air} = \frac{A\rho_{ice}}{s_{op}^{*}P_0}\left(\frac{s_{cl}(z_{COD})P_{cl}(z_{COD})}{\rho_{COD}} - \frac{s_{cl}(z)P_{cl}(z)}{\rho(z)}\right) \quad (1)$$ where

A is the accumulation rate (0.10 m ice yr^{-1}), z_{COD} is the full close-off depth, ρ_{ice} is the density of ice (0.921 g cm^{-3}), s_{op}^{*} is the effective open porosity, s_{cl} is the closed porosity, and P_0 and P_{cl} is the enhanced pressure due to firn compaction in closed bubbles. Other variables are expressed in Table 1.

2.3 CH_4 in closed bubbles and total air content measurements

The Cryosphere Discuss., https://doi.org/10.5194/tc-2019-17
Manuscript under review for journal The Cryosphere
Discussion started: 5 March 2019

CH_4 mole fraction in the (closed) air bubbles in the firn ice was measured at Seoul National University by a wet extraction method which extracts air from the ice by thawing and refreezing (Yang et al., 2017). 124 discrete firn ice samples (cross section of 8.5 cm × 3 cm, length of 3 cm, ~35 g) were prepared from 4 different depth intervals in the lock-in zone (54.59-55.34, 58.11-59.05, 59.86-60.55, 64.02-65.25 m). All ice samples were cut and trimmed by ~2.5 mm with a band saw to remove the surface ice. Then, the ice samples were inserted into the glass flasks attached to the gas extraction line. The pump system evacuated air in the flask in the cooled ethanol bath at -70 °C for 20 min. After the pressure dropped below 0.2 mTorr, the ice samples in the glass flask were melted and air in the bubbles were extracted. After the melting was finished, we refroze the ice using a cooled ethanol bath to release the gas dissolved in the ice melt. Finally, the extracted air was injected into the sample loop of the gas chromatograph equipped with a flame ionization detector (FID). The calibration curve of the GC-FID was calculated by standard air with the CH_4 mole fraction of 895 ppbv on the NOAA04 scale (Dlugokencky et al., 2005).

2.4 Analysis for stable isotopes of ice

After the measurement of the CH_4 mole fraction in air, the melt water was put into cleaned 125 ml bottles and analyzed for water stable isotope ratios at Korea Polar Research Institute (KOPRI) using a Cavity Ring-Down Spectroscopy (CRDS, L1102-i, Picarro, USA) system. The data are here presented as δ-notations ($\delta^{18}O(‰)=((^{18}O/^{16}O)_{sample}/(^{18}O/^{16}O)_{VSMOW}-1)\times1000$, $\delta D(‰)=((^{2}H/^{1}H)_{sample}/(^{2}H/^{1}H)_{SMOW}-1)\times1000)$). The firn ice melt was filled into a 400 μl insert in a 2 ml glass vial using a syringe filter. The auto sampler transported the ice melt samples in the insert to the vaporizer about 180 nl at a time. The samples with the liquid state were transferred to the cavity after being converted into the water vapor in a vaporizer at 110 °C. The measurement precision evaluated by measuring an in-house standard repeatedly (n=12) was 0.08‰ for $\delta^{18}O$ and 0.3‰ for δD (1 sigma standard deviations).

2.5 X-ray firn density measurement

We obtained high-resolution density data using the X-ray transmission method reported by Hori et al. (1999) for the firn ice at various depth intervals. This method is advantageous because it can measure continuously and

The Cryosphere Discuss., https://doi.org/10.5194/tc-2019-17
Manuscript under review for journal The Cryosphere
Discussion started: 5 March 2019

non-destructively. The X-ray beam penetrates the ice samples and the detector on the opposite side analyzes the intensity of the beam. To make equal thickness for each core section, upper and side parts of the half circle-shape core were shaved by a microtome. After putting the precut ice core on a rack, we set the rate of measurement at 50 mm min^{-1}, and finally obtained 1mm-resolution density data.

3 Results

3.1 Layered stratigraphy

We examined a snow pit, located 10 m away from the main ice core borehole, 2 years after drilling to understand the physical properties such as layers, density, and ice grain size of the upper firn at Styx site. We scratched the snow wall by hand to remove soft layers and enhance the visibility of hard layers (Fig. 2a). The soft layers have low density and are presumed to be depth hoar coarse, and the hard ones are wind crusts with high density (Fig. 2b). The alternating layers repeat with intervals of few centimeters to 20 centimeters. The top boundaries of the hard layers are sharp and extend horizontally about a meter, but the bottom boundaries are not well defined due to gradual density changes. 10 cm-resolution density data were obtained by a density cutter (Proksch et al., 2016). The density is low in coarse-grained layers, while it is high in fine-grained layers (Fig. 2b-d).

3.2 Firn gas sampling and the age of firn air

We calibrate the depth-diffusivity profile in the model using trace gases with a well-known atmospheric history (Buizert et al., 2012a; Trudinger 1997; Rommelaere 1997). The atmospheric time series from well-dated firn air (Etheridge et al. 1996, 1998) and instrument measurement records (NOAA; https://www.esrl.noaa.gov/) were used for calibration. The simulated mole fraction profiles match well with the observations (Fig. 3). CO_2, CH_4, SF_6 and $\delta^{15}N\text{-}N_2$ distributions in firn air were modeled. The model does not include thermal fractionation, and therefore provides a poor fit to the $\delta^{15}N\text{-}N_2$ data in the upper firn where seasonal temperature gradients fractionate the gases. The firn air age (black curves in Fig. 3) slowly increases with depth at the diffusive zone because it mixes with fresh atmospheric air on the surface mostly by molecular diffusion (Blunier and Schwander, 2000). In contrast, the firn air age rapidly increases with the same rate of the surrounded ice age in the LIZ.

The lowest CO_2 mole fraction of 305.18 ppmv at depth of 64.8 m corresponds to the year of 1927 or mean age of 89 years (relative to sampling year 2014) on the Law Dome ice core record (MacFarling Meure et al., 2006). We also obtained the CH_4 mole fraction of 943.36 ppbv at the same depth, which corresponds to an age of 88 years (MacFarling Meure et al., 2006) (Figs. 3a, 3b). Each gas has different modeled ages because their diffusivities are different. Only few studies have reported firn air ages older than 89 years: 93 years from the South Pole (Severinghaus et al., 2001) and 121 years from Megadunes (Severinghaus et al., 2001; Fig. 1). These sites are located inland Antarctica and have low annual mean temperatures and low snow accumulation rates (Table 1). Firn densification takes a long time if snow accumulation is low, therefore the firn air can be preserved for a long time without being trapped. In contrast, Styx site is located near the coast and has relatively high snowfall, and therefore the age of 89 years is very unusual. Sites of comparable climate characteristics typically have an oldest firn air age of around 40 years. This indicates that there may be other factors that can permit preservation of the old firn air at Styx Glacier.

3.3 Density layering and its influence on bubble trapping

Firn density is the primary control on the bubble close-off process, and therefore density layering leads to staggered bubble trapping, with high-density layers closing off before low-density ones (Etheridge et al. 1992, Mitchell et al. 2015, Rhodes et al. 2016).

Because the atmospheric CH_4 mole fraction has increased during the last century, we may obtain information on the timing of the bubble close-off from the CH_4 mole fraction of the air trapped in closed bubbles ($[CH_4]_{cl}$). In this study, we used the $[CH_4]_{cl}$ and total air content of the firn ice as indicators of the close-off process. The density and $[CH_4]_{cl}$ show an anti-correlation (Fig. 5). High-density layers reach the lock-in and close-off densities at shallower depths than low-density layers (Fig. 5). Thus, air bubbles are trapped at shallower depths in high-density layers. Early trapped bubbles preserve older air with lower greenhouse gas mole fractions. Meanwhile, higher air content is expected in the high-density layers, in which open porosity is small and closed porosity is large (Fig. 5). However, we cannot entirely exclude the possibility of some post-coring bubble close-off. High open porosity in low-density layers may have more chances to trap modern ice storage air, which has

The Cryosphere Discuss., https://doi.org/10.5194/tc-2019-17
Manuscript under review for journal The Cryosphere
Discussion started: 5 March 2019

higher mole fraction of CH_4 than atmospheric background levels.

Figure 5a shows $[CH_4]_{cl}$ and total air contents in the LIZ of the Styx firn. $[CH_4]_{cl}$ generally decreases with depth and the variations are stabilized at a deeper layer, while the total air content generally increases with depth. The $[CH_4]_{cl}$ greater than CH_4 mole fraction in neighboring firn air (green line in Fig. 5a) indicates part of bubbles formed after coring and increased the $[CH_4]_{cl}$, as previous studies also observed (Mitchell et al., 2015; Rhodes et al., 2013). Most of $[CH_4]_{cl}$ data show large cm-scale variations (Fig. 5). The highs and lows of $[CH_4]_{cl}$ repeat with cycles of 6 cm to 24 cm (Fig. 5b). Note that the layering observed in the snow pit likewise showed irregular intervals (Fig. 2b). From the layer spacing, we conclude that bubble trapping at Styx is not controlled by annual layers (Section 4), as was observed at Law Dome (Etheridge et al. 1992).

The evolution of CH_4 in the closed porosity may give information on how the snow layers can make inhomogenous records and how the gas age distribution is determined in ice core studies (Fourteau et al. 2017, www.clim-past.net/13/1815/2017/). However, the details are beyond the scope of this study and we will focus on the firn air age in the open porosity.

3.4 High-resolution firn density measurements

The X-ray measurements show highly variable density on cm scales. We converted the high-resolution density to total porosity using the following equation:

$$\Phi_{total} = 1 - \frac{\rho}{\rho_{ice}} \quad (3)$$

where ρ = density of porous ice; ρ_{ice} = density of bubble-free ice (919 kg m^{-3}); and Φ = porosity.

At Styx Glacier, the shallowest depth, where the running mean of total porosity with a 1 cm-thick window reaches below 0.1, is 48.1 m (Figs. 6a and 6b). It is approximately 4.3 m shallower than the LID of 52.4 m defined by the firn air $\delta^{15}N\text{-}N_2$. Meanwhile, the deepest point, where the running mean (with a 1 cm-thick window) becomes less than 0.1, is at 63.7 m (Figs. 6a and 6c), which is shallower than the COD of 64.8 m defined by the deepest successful firn pumping depth. Although the LID and COD from the density data are different from those defined by firn air data, the thickness of LIZ from density data is comparable to that from firn air analysis (between two blue lines in Fig. 6). The offsets of the LIZ about 1-4 m between those from total porosity and the firn air measurement may be due to the fact that actual critical porosity may be variable and depend on study sites, perhaps depending on horizontal snow density variations and the horizontal extent of diffusion-impeding layers. In spite of the possibilities of error, the similarity in the LIZ thicknesses from the two methods support the idea that the large variations of density can increase the LIZ thickness by shallowing LID and/or deepening the COD. The thick LIZ eventually permits storing old firn air at Styx (Table 1). We demonstrate here that the snow density variability is an important factor in determining the firn air age. We suggest that sites with higher density variations at the LIZ have a high possibility of a thick LIZ and therefore old firn air, even in warm, high-precipitation coastal climates.

4 Discussions

To quantitatively compare density variability of Styx snow with those at other glacier sites, we may use the standard deviation of densities (σ_ρ) near the mean air-isolation density (Hörhold et al., 2011; Martinerie et al., 1992). The mean density at the mean air-isolation depth (ρ_{crit}) can be related to mean annual temperature (T in Kelvin) using the following equation, which is empirically obtained from air content measurements (Martinerie et al., 1992):

$$\rho_{\mathrm{crit}} = \left(\frac{1}{\rho_{ice}} + 7.6 \times 10^{-4} \times T - 0.057\right)^{-1} \quad (4),$$

where ρ_{ice} is the density of bubble-free pure ice.

Although this equation cannot provide exact ρ_{crit}, we can take advantage in estimating the density at LIZ without gas chemistry data (Hörhold et al., 2011). Using the Styx high-resolution X-ray density data at depth interval of 43.13-66.97 m, we calculated the standard deviation of densities (σ_ρ). For each σ_ρ, we used 1000 density data points (Fig. 7) as Hörhold et al. (2011) did (Table 2). At Styx, ρ_{crit} is 821.68 kg m^{-3} according to equation (4), and the standard deviation of densities at ρ_{crit} (σ_ρ, ρ_{crit}) is 19.33 ± 1.87 kg m^{-3}, which is greater than those in the other previously studied sites (Fig. 7, Table 2). The high σ_ρ, ρ_{crit} at Styx likely facilitates the thick LIZ and old firn air. A high snow accumulation rate may not allow old firn air ages for a certain LIZ thickness. Thus, σ_ρ,

The Cryosphere Discuss., https://doi.org/10.5194/tc-2019-17
Manuscript under review for journal The Cryosphere
Discussion started: 5 March 2019

The Cryosphere Discussions
Open Access

ρ_{crit} divided by a snow accumulation rate (A) can be a better indicator of the range of air ages. The Styx (σ_ρ, ρ_{crit} / A) is also greater than other studied sites (Table 2).

A high-density (low-density) layer at surface may become a low-density (high-density) layer (Freitag et al., 2004; Fujita et al., 2009) at density of 600-650 kg m^{-3}, which occurs at shallower depths than LIZ (Hörhold et al., 2011). Thus, vertical snow layering at surface may not directly give information about density variability at LIZ (Hörhold et al., 2011). However, conditions for snow layering at the surface still may give us clues on the density variability at LIZ. The conditions may include redistribution of snow by wind and formation of wind and/or radiation crusts (Martinerie et al., 1992; Hörhold et al., 2011). To test the possibility of seasonal causes, we analyzed stable isotopes of surface snow ($\delta^{18}O$) because the surface $\delta^{18}O$ generally follows seasonal variation (depleted in winter and enriched in summer). Figures 2e and 2f show the stable isotope profiles of snow ($\delta^{18}O$) at Styx Glacier, which are apart by ~100 m; one is from a snow pit made in 2014 and the other is from the main ice core drilled in 2014. The $\delta^{18}O$ profiles commonly show cycles with intervals of ~40 cm per year, given that local maxima of $\delta^{18}O$ indicate summer, and minima winter layers. Meanwhile, the repetition of the density layers has twenty cycles (high and low density layer pairs) in the top 180 cm depth at the snow pit (Fig. 2b). Applying the snow accumulation rate of ~40 cm y^{-1} in recent years, the density layers have 4~5 cycles y^{-1}, indicating that the formation of snow density layers is mainly controlled by non-seasonal factors.

A blizzard occurred during the ice coring campaign in December of 2014. We observed that the blizzard strongly reworked the surface snow. The Automatic Weather System (AWS) installed within 10 m from the borehole site show that blizzard events (wind speed > 15 m s^{-1}) took place on December 29 in 2015, May 23, June 26, August 17, and September 7 in 2016 (Fig. 8). The number of blizzard events in a year is similar to the mean density layer cycle of 4~5 y^{-1}. Although Blizzard occurs more frequently in winter, the frequency of 5 yr^{-1} is comparable to the number of the density layer cycles of 4~5 yr^{-1}. At the time intervals, westerly wind prevailed. When redeposited by a blizzard event, particles of snow can be sorted (Sepp Kipfstuhl, personal communications) and following solar radiation and temperature gradient may facilitate diagenesis of the snow layers (Alley, 1988; Fegyveresi et al., 2018). During the diagenesis processes, fine and coarse flake layers may form high-density and low-density layers, respectively.

5 Conclusions and implications

About 89-year-old firn air was found at Styx Glacier, East Antarctica, located near the Ross Sea coast. This is of great scientific interest because such old firn air is commonly only found in the inland sites such as the South Pole and Megadunes. The thickness of Styx LIZ is relatively greater than those in other sites where snow accumulation and temperature are similar. The thicker LIZ made the Styx firn layer preserve old firn air because the age of stagnant firn air rapidly increases with depth in the LIZ as air exchange with the atmosphere has stopped. We hypothesized that the high snow density variations at the LIZ of Styx Glacier made the thick LIZ and old firn air. To test the hypothesis, we conducted high-resolution X-ray density measurements. We argue that the thick LIZ is related to the high density variations at Styx Glacier. We also examined why high snow density variability developed at Styx site. The effect of strong wind (e.g., blizzards) may facilitate the density layer formation. It is likely that old firn air (>55 years) can be found in areas where climatological conditions are favorable for high snow density variations at LIZ even when the sites are located near the coast. We may take advantage in sampling and transportation from the coastal sites, because logistics is easier for those sites.

Acknowledgements. This study was supported by Korea Polar Research Institute (PE 18040) and National Research Foundation of Korea (NRF-2018R1A2B3003256).

References

Alley, R. B.: Concerning the Deposition and Diagenesis of Strata in Polar Firn, Journal of Glaciology, 34, 283-290, http://dx.doi.org/10.3189/s0022143000007024, 1988.

Battle, M. O., Severinghaus, J. P., Sofen, E. D., Plotkin, D., Orsi, A. J., Aydin, M., Montzka, S. A., Sowers, T., and Tans, P. P.: Controls on the movement and composition of firn air at the West Antarctic Ice Sheet Divide, Atmospheric Chemistry and Physics Discussions, 11, 18633-18675, http://dx.doi.org/10.5194/acpd-11-18633-2011, 2011.

Blunier, T. and Schwander, J.: Gas enclosure in ice: age difference and fractionation, in: Physics of Ice Core Records, edited by: Hondoh, T., Hokkaido University Press, Sapporo, 307–326, 2000.

Buizert, C., Martinerie, P., Petrenko, V. V., Severinghaus, J. P., Trudinger, C. M., Witrant, E., Rosen, J. L., Orsi, A. J., Rubino, M., Etheridge, D. M., Steele, L. P., Hogan, C., Laube, J. C., Sturges, W. T., Levchenko, V. A., Smith, A. M., Levin, I., Conway, T. J., Dlugokencky, E. J., Lang, P. M., Kawamura, K., Jenk, T. M., White, J.W. C., Sowers, T., Schwander, J., and Blunier, T.: Gas transport in firn: multiple-tracer characterisation and model intercomparison for NEEM, Northern Greenland, Atmos. Chem. Phys., 12, 4259–4277, doi:10.5194/acp-12-4259-2012, 2012a.

Buizert, C.: The influence of firn air transport processes and radiocarbon production on gas records from polar firn and ice, PhD, Faculty of Science, University of Copenhagen, Denmark, Copenhagen, 175 pp., 2012b.

Buizert, C. and Severinghaus, J. P.: Dispersion in deep polar firn driven by synoptic-scale surface pressure variability, The Cryosphere, 10, 2099–2111, https://doi.org/10.5194/tc-10-2099-2016, 2016.

Craig, H., Horibe, Y., and [illegible] S.: Gravitational separation of gases and isotopes in polar ice caps, Science, 242, 1675–1678, 1988.

Dlugokencky, E. J., Myers, R. C., Lang, P. M., Masarie, K. A., Crotwell, A. M., Thoning, K. W., Hall, B. D., Elkins, J. W., and Steele, L. P.: Conversion of NOAA atmospheric dry air CH4 mole fractions to a gravimetrically prepared standard scale, J. Geophys. Res., 110, D18306, https://doi.org/10.1029/2005JD006035, 2005.

Etheridge, D. M., Pearman, G. I., and Fraser, P. J.: Changes in tropospheric methane between 1841 and 1978 from a high accumulation-rate Antarctic ice core, Tellus B, 44, 282–294, doi:10.1034/j.1600-

The Cryosphere Discuss., https://doi.org/10.5194/tc-2019-17
Manuscript under review for journal The Cryosphere
Discussion started: 5 March 2019

The Cryosphere Discussions

0889.1992.t01-3-00006.x, 1992.

Etheridge, D. M., Steele, L. P., Langenfelds, R. L., Francey, R. J., Barnola, J. M., and Morgan, V. I.: Natural and anthropogenic changes in atmospheric CO_2 over the last 1000 years from air in Antarctic ice and firn, J. Geophys. Res., 101, 4115–4128, doi:10.1029/95jd03410, 1996.

Etheridge, D. M., Steele, L. P., Francey, R. J. and Langenfelds, R. L.: Atmospheric methane between 1000 A.D. and present: Evidence of anthropogenic emissions and climatic variability, Journal of Geophysical Research, 103(D13), 15979, doi:10.1029/98JD00923, 1998.

Fegyveresi, J. M., Alley, R. B., Muto, A., Orsi, A. J., and Spencer, M. K.: Surface formation, preservation, and history of low-porosity crusts at the WAIS Divide site, West Antarctica, The Cryosphere, 12, 325-341, http://dx.doi.org/10.5194/tc-12-325-2018, 2018.

Freitag, J., Wilhelms, F., and Kipfstuhl, S.: Microstructure dependent densification of polar firn derived from X-ray microtomography, J. Glaciol., 50, 243–250, 2004.

Fujita, S., Okuyama, J., Hori, A., and Hondoh, T.: Metamorphism of stratified firn at dome fuji, antarctica: A mechanism for local insolation modulation of gas transport conditions during bubble close off, J. Geophys. Res., 114, F03023, doi:10.1029/2008JF001143, 2009.

Goujon, C., Barnola, J. M., and Ritz, C.: Modeling the densification of polar firn including heat diffusion: Application to closeoff characteristics and gas isotopic fractionation for Antarctica and Greenland sites, J. Geophys. Res.-Atmos, 108, 4792, doi:10.1029/2002JD003319, 2003.

Gregory, S. A., Albert, M. R., and Baker, I.: Impact of physical properties and accumulation rate on pore close-off in layered firn, The Cryosphere, 8, 91-105, http://dx.doi.org/10.5194/tc-8-91-2014, 2014.

Han, Y., Jun, S. J., Miyahara, M., Lee, H.-G., Ahn, J., Chung, J. W., Hur, S. D., and Hong, S. B.: Shallow ice-core drilling on Styx glacier, northern Victoria Land, Antarctica in the 2014-2015 summer, Journal of the Geological Society of Korea, 51, 343-355, 2015

Hörhold, M. W., Kipfstuhl, S., Wilhelms, F., Freitag, J., and Frenzel, A.: The densification of layered polar firn, Journal of Geophysical Research: Earth Surface, 116, http://dx.doi.org/10.1029/2009jf001630, 2011.

Hori, A., Tayuki, K., Narita, H., Hondoh, T., Fujita, S., Kameda, T., Shoji, H., Azuma, N., Kamiyama, K., Fujii, Y., Motoyama, H., and Watanabe, O.: A detailed density profile of the Dome Fuji (Antarctica) shallow ice core by X-ray transmission method, Annals of Glaciology, 29, 211-214, http://dx.doi.org/10.3189/172756499781821157, 1999.

Johnsen, S. J., Clausen, H. B., Cuffey, K. M., Hoffmann, G., Schwander, J., and Creyts, T.: Diffusion of stable isotopes in polar firn and ice: the isotope effect in firn diffusion, in: Physics of Ice Core Records, edited by: Hondoh, T., vol. 159, 121–140, Hokkaido University Press, Sapporo, Japan, 2000.

Kawamura, K., Severinghaus, J. P., Albert, M. R., Courville, Z. R., Fahnestock, M. A., Scambos, T., Shields, E., and Shuman, C. A.: Kinetic fractionation of gases by deep air convection in polar firn, Atmospheric Chemistry and Physics, 13, 11141-11155, http://dx.doi.org/10.5194/acp-13-11141-2013, 2013.

Landais, A., Barnola, J.M., Kawamura, K., Caillon, N., Delmotte, M., Van Ommen, T., Dreyfus, G., Jouzel, J., Masson-Delmotte, V., Minster, B., Freitag, J., Leuenberger, M., Schwander, J., Huber, C., Etheridge, D., and Morgan, V.: Firn-air δ15N in modern polar sites and glacial–interglacial ice: a model-data mismatch during glacial periods in Antarctica?, Quaternary Science Reviews, 25, 49-62, http://dx.doi.org/10.1016/j.quascirev.2005.06.007, 2006.

Laube, J. C., Hogan, C., Newland, M. J., Mani, F. S., Fraser, P. J., Brenninkmeijer, C. A. M., Martinerie, P., Oram, D. E., Röckmann, T., Schwander, J., Witrant, E., Mills, G. P., Reeves, C. E., and Sturges, W. T.: Distributions, long term trends and emissions of four perfluorocarbons in remote parts of the atmosphere and firn air, Atmos. Chem. Phys., 12(9), 4081-4090, 2012.

MacFarling-Meure, C., Etheridge, D., Trudinger, C., Steele, P., Langenfelds, R., van Ommen, T., Smith, A., and Elkins, J.: Law Dome CO2, CH4 and N2O ice core records extended to 2000 years BP, Geophys. Res. Lett., 33, L14810, doi:10.1029/2006GL026152, 2006.

Martinerie, P., Raynaud, D., Etheridge, D. M., Barnola, J. M., and Mazaudier, D.: Physical and Climatic Parameters which Influence the Air Content in Polar Ice, Earth Planet. Sc. Lett., 112, 1–13, doi:10.1016/0012-821X(92)90002-D, 1992.

Mitchell, L. E., Buizert, C., Brook, E. J., Breton, D. J., Fegyveresi, J., Baggenstos, D., Orsi, A., Severinghaus, J., Alley, R. B., Albert, M., Rhodes, R. H., McConnell, J. R., Sigl, M., Maselli, O., Gregory, S., and Ahn, J.: Observing and modeling the influence of layering on bubble trapping in polar firn, J. Geophys. Res.-Atmos., 120, 2558–2574, https://doi.org/10.1002/2014JD022766, 2015.

Petit, J. R., Jouzel, J., Raynnaud, D., Barkov, N. I., Barnola, J.-M., Basile, I., Bender, M., Chappellaz, J., Davis, M., Delaygue, G., Delmotte, M., Kotlyakov, V. M., Legrand, M., Lipenkov, V. Y., Lorius, C., Pepin, L., Ritz, C., Saltzman, E., and Stievenard, M.: Climate and atmospheric history of the past 420 000 years from the Vostok ice core, Antarctica, Nature, 399, 429–436, 1999.

Proksch, M., Rutter, N., Fierz, C., and Schneebeli, M.: Intercomparison of snow density measurements: bias, precision, and vertical resolution, The Cryosphere, 10, 371–384, doi:10.5194/tc-10-371-2016, 2016.

Rhodes, R. H., Fain, X., Stowasser, C., Blunier, T., Chappellaz, J., McConnell, J. R., Romanini, D., Mitchell, L. E., and Brook, E. J.: Continuous methane measurements from a late Holocene Greenland ice core: atmospheric and in-situ signals, Earth Planet. Sc. Lett., 368, 9–19, 2013.

Rhodes, R. H., Faïn, X., Brook, E. J., McConnell, J. R., Maselli, O. J., Sigl, M., Edwards, J., Buizert, C., Blunier, T., Chappellaz, J., and Freitag, J.: Local artifacts in ice core methane records caused by layered bubble trapping and in situ production: a multi-site investigation, Clim. Past, 12, 1061–1077, doi:10.5194/cp-12-1061- 2016, 2016.

Rommelaere, V., Arnaud, L., and Barnola, J. M.: Reconstructing recent atmospheric trace gas concentrations from polar firn and bubbly ice data by inverse methods, J. Geophys. Res.-Atmos., 102, 30069–30083, doi:10.1029/97JD02653, 1997.

Schaller, C. F.., Freitag, J., and Eisen, O.: Critical porosity of gas enclosure in polar firn independent of climate, Climate of the Past, 13, 1685-1693, http://dx.doi.org/10.5194/cp-13-1685-2017, 2017.

Schwander, J.: The transformation of snow to ice and the occlusion of gases, Environ. Rec. Glaciers Ice Sheets, 8, 53–67, 1989.

Schwander, J., Barnola, J.-M., Andrié, C., Leuenberger, M., Ludin, A., Raynaud, D., and Stauffer, B.: The age of the air in the firn and the ice at Summit, Greenland, Journal of Geophysical Research: Atmospheres, 98, 2831-2838, http://dx.doi.org/10.1029/92jd02383, 1993.

Severinghaus, J. P., Grachev, A., and Battle, M.: Thermal fractionation of air in polar firn by seasonal temperature gradients, Geochem. Geophy. Geosy., 2, 1048, doi:10.1029/2000GC000146, 2001.

Severinghaus, J. P., Albert, M. R., Courville, Z. R., Fahnestock, M. A., Kawamura, K., Montzka, S. A., Mühle, J., Scambos, T. A., Shields, E., Shuman, C. A., Suwa, M., Tans, P., andWeiss, R. F.: Deep air convection in the firn at a zero-accumulation site, central Antarctica, Earth Planet. Sc. Lett., 293, 359–367, https://doi.org/10.1016/j.epsl.2010.03.003, 2010.

Sowers, T., Bender, M., Raynaud, D., and Korotkevich, Y. S.: Delta n-15 of n2 in air trapped in polar ice – a tracer of gas-transport in the firn and a possible constraint on ice age-gas age-differences, J. Geophys. Res.-Atmos., 97, 15683–15697, 1992.

Trudinger, C. M., Enting, I. G., Etheridge, D. M., Francey, R. J., Levchenko, V. A., Steele, L. P., Raynaud, D., and Arnaud, L.: Modeling air movement and bubble trapping in firn, J. Geophys. Res.-Atmos., 102, 6747–6763, doi:10.1029/96JD03382, 1997.

Witrant, E., Martinerie, P., Hogan, C., Laube, J. C., Kawamura, K., Capron, E., Montzka, S. A., Dlugokencky, E. J., Etheridge, D., Blunier, T., and Sturges, W. T.: A new multi-gas constrained model of trace gas non-homogeneous transport in firn: evaluation and behaviour at eleven polar sites, Atmos. Chem. Phys., 12, 11465–11483, doi:10.5194/acp-12-11465-2012, 2012.

Yang, J. W., Ahn, J., Brook, E. J., and Ryu, Y.: Atmospheric methane control mechanisms during the early Holocene, Climate of the Past, 13, 1227-1242, http://dx.doi.org/10.5194/cp-13-1227-2017, 2017.

Yang, J. W., Han, Y., Orsi, A. J., Kim, S. J., Han, H., Ryu, Y., Jang, Y., Moon, J., Choi, T., Hur, S. D., and Ahn, J.: Surface temperature in twentieth century at the Styx Glacier, northern Victoria Land, Antarctica, from borehole thermometry. Geophysical Research Letters., 2018.

The Cryosphere Discuss., https://doi.org/10.5194/tc-2019-17
Manuscript under review for journal The Cryosphere
Discussion started: 5 March 2019

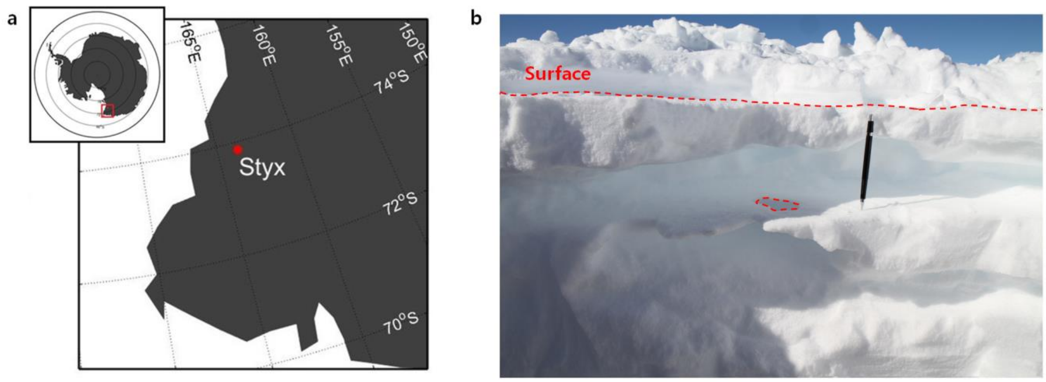

Figure 1. Location map of study site, Styx Glacier, Antarctica (a) and a photo of surface snow density layers (b). The thickness of snow density layers vary horizontally. The top boundaries of high-density layers are sharp (horizontal red-dashed line). A hole on a high-density layer surface is indicated by a red-dashed circle.

The Cryosphere Discuss., https://doi.org/10.5194/tc-2019-17
Manuscript under review for journal The Cryosphere
Discussion started: 5 March 2019

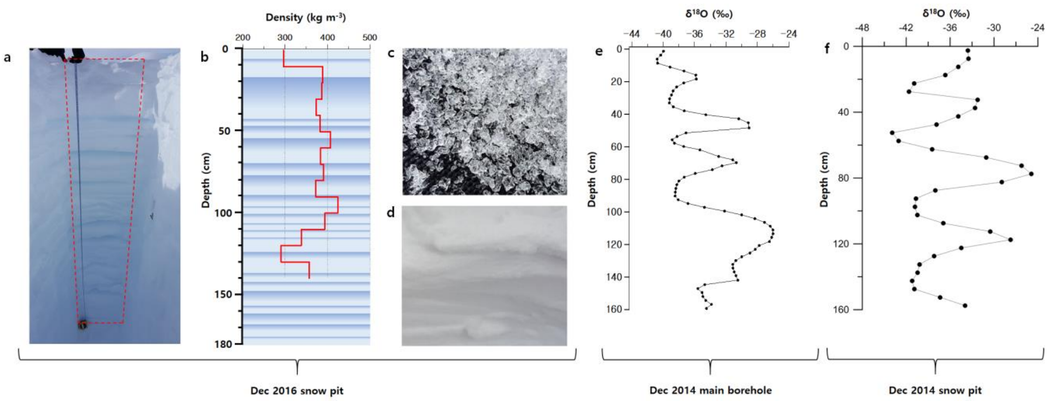

Figure 2. The snow-pit photos at Styx Glacier. (a) The snow-pit with dimensions of 280×65×220 cm (length×width×height). (b) The illustration of qualitatively-defined hard (high-density) and soft (low-density) layers with a 10 cm-resolution density profile. (c) Coarse grains observed in a soft layer. (d) Fine grains observed in a hard layer. Stable isotope ratio ($\delta^{18}O$) of snow profiles at the main core (e) and a snow-pit 100 m away from the main ice core borehole (f).

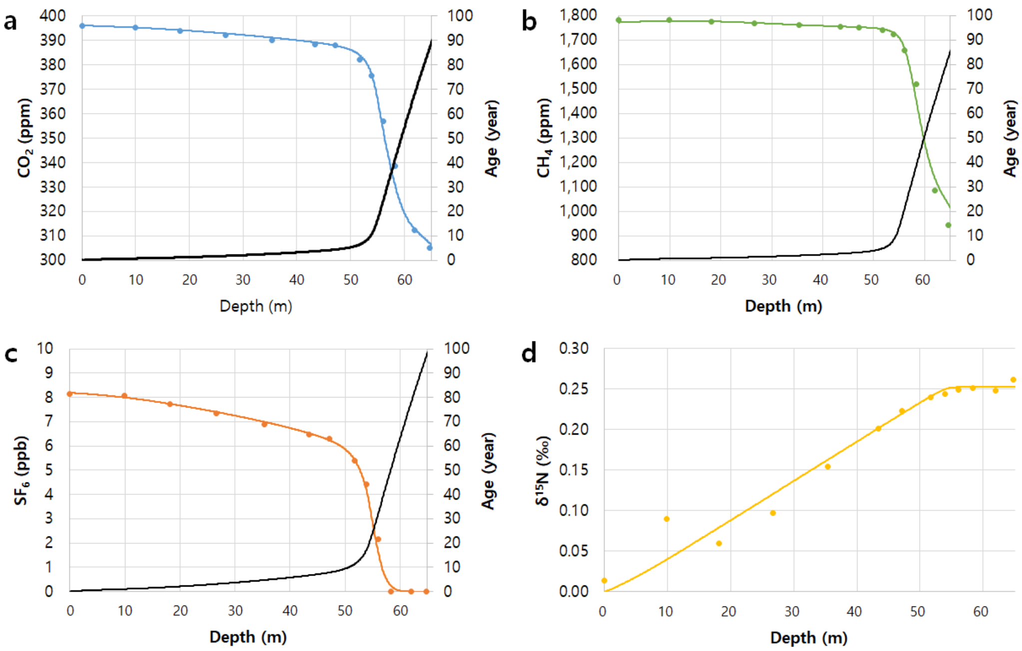

Figure 3. CO_2, CH_4, SF_6 mole fractions and $\delta^{15}N$ of N_2 measurements (circles), and model results (solid line) for the Styx firn air (air in open porosity). Black lines are modeled ages for the gas species.

The Cryosphere Discuss., https://doi.org/10.5194/tc-2019-17
Manuscript under review for journal The Cryosphere
Discussion started: 5 March 2019

The Cryosphere
Discussions
Open Access

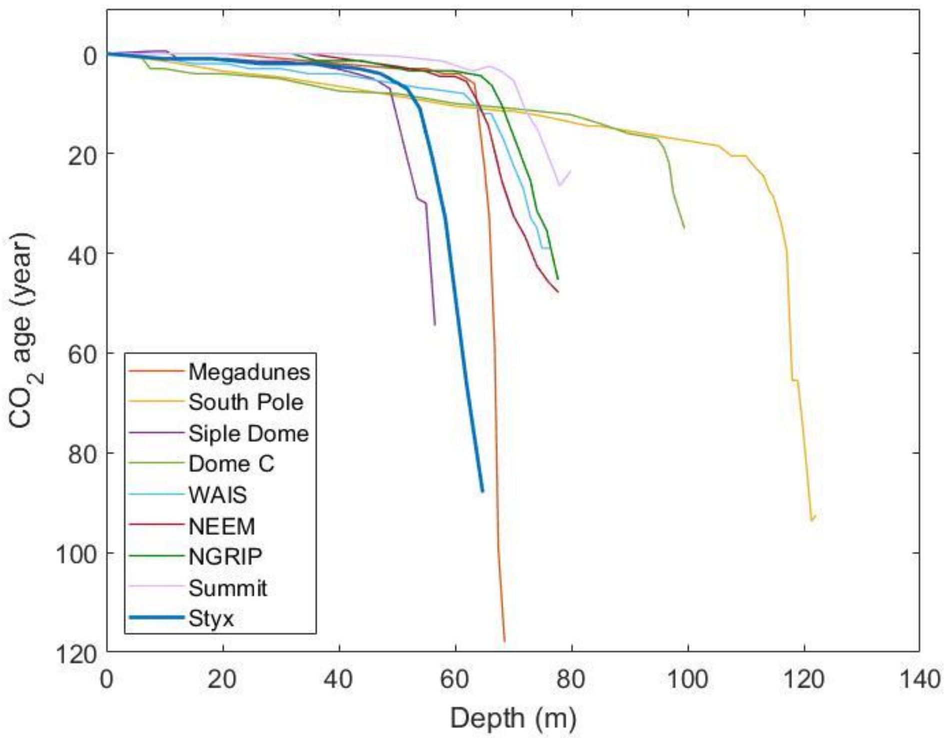

Figure 4. Comparison of CO_2 ages at several firn air sampling sites in Antarctica and Greenland. Old firn air (>55 years) is reported only in inland sites, where temperatures and snow accumulation rates are relatively low. However, 89-year old firn air was observed at Styx Glacier, where coast is near and snow accumulation rates are high.

The Cryosphere Discuss., https://doi.org/10.5194/tc-2019-17
Manuscript under review for journal The Cryosphere
Discussion started: 5 March 2019

The Cryosphere Discussions
Open Access
EGU

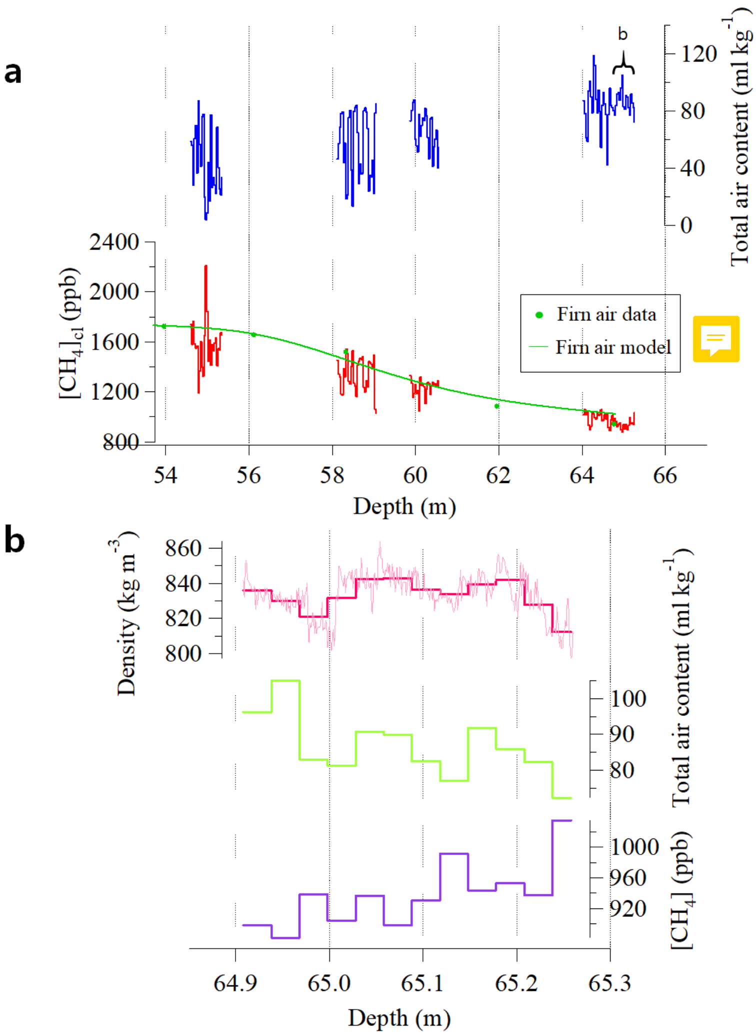

Figure 5. (a) CH_4 mole fraction in closed pores ([CH_4]$_{cl}$)(red line) and total air content (air volume per ice weight) (blue line) in the lock-in zone. Green line indicates CH_4 mole fraction in open pores. (b) Comparison of density with [CH_4]$_{cl}$ and total air content near COD.

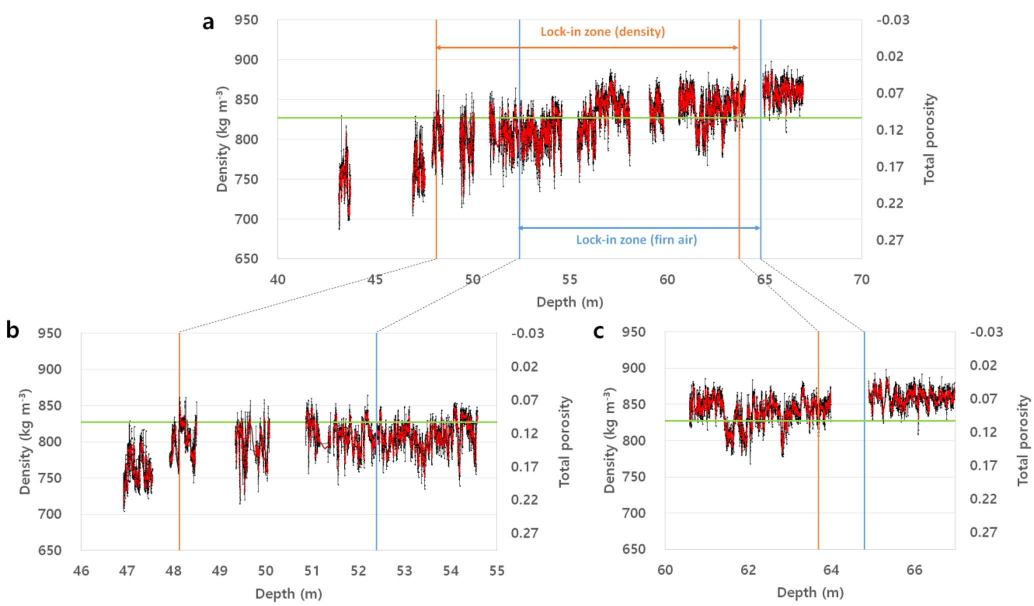

Figure 6. X-ray high-resolution density data obtained from the lock-in zone. (b) and (c) are enlarged portion of (a). Black lines show individual density data, while the red lines 1-cm running means. Blue and orange lines represent the boundaries of the LIZ estimated from the gas compositions (between two vertical blue lines) and the critical porosity measurements (between two orange vertical lines), respectively.

The Cryosphere Discuss., https://doi.org/10.5194/tc-2019-17
Manuscript under review for journal The Cryosphere
Discussion started: 5 March 2019

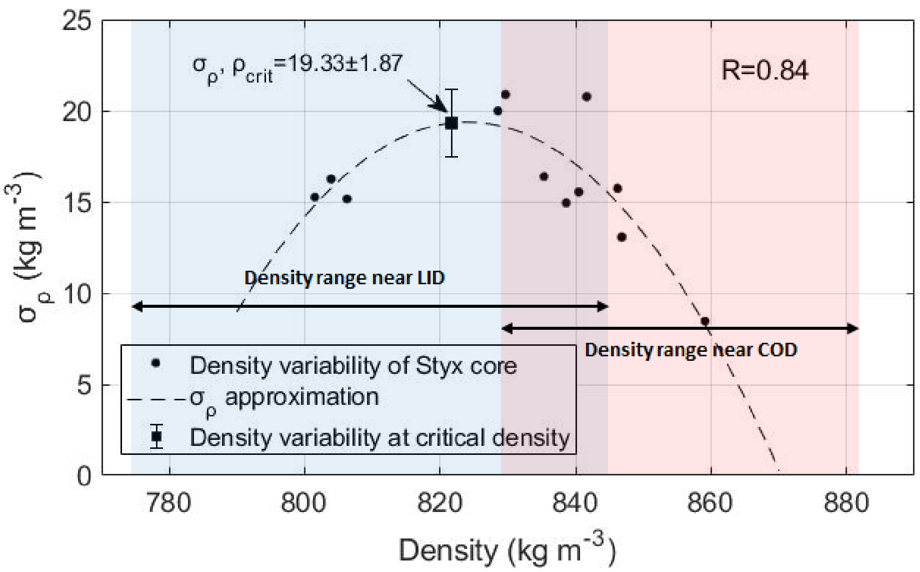

Figure 7. Density variability calculated from 1000 depth points and their average density. The standard deviation at the critical density (821.68 kg m^{-3}) calculated from the approximate secondary equation (R=0.84) is 19.33±1.87 kg m^{-3}. The blue and red areas are the density ranges near the LID (52.38-52.48 m) and the COD (64.91-65.01 m), respectively.

The Cryosphere Discuss., https://doi.org/10.5194/tc-2019-17
Manuscript under review for journal The Cryosphere
Discussion started: 5 March 2019

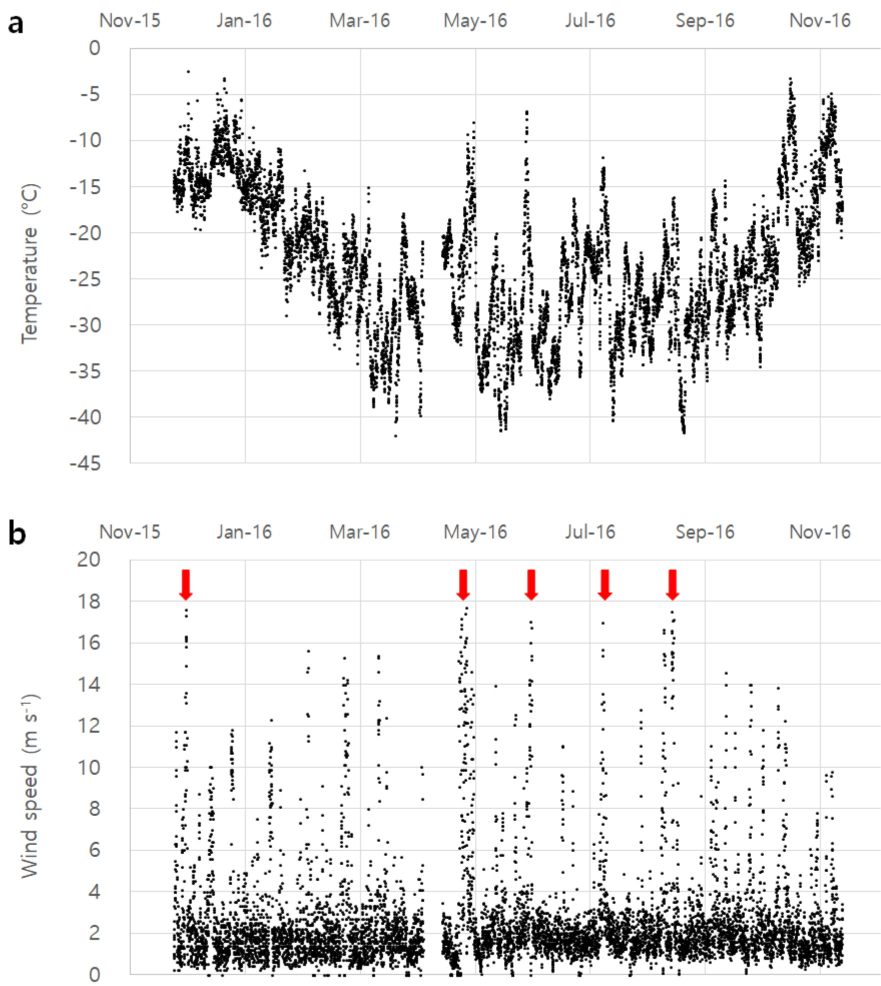

Figure 8. Surface air temperature (a) and wind speed (b) data from AWS (Automatic Weather System) at Styx Glacier during December 2015 to December 2016. Red arrows indicate blizzard events.

Table 1. Glaciological characteristics of Styx Glacier and other firn air sampling sites.

Site	T (℃)	A (cm ice yr^{-1})	Firn air age (year)	LID (m)	COD (m)	LIZ thickness (m)	References
Styx	-31.7	10	89	52.4	64.8	12.4	This study, Yang et al. (2018)
Megadunes	-49	~0	121	64.5	68.5	4	Severinghaus et al. (2010)
South Pole	-51.0	8	93	115	125	10	Severinghaus et al. (2001)
Siple Dome	-25.4	13	55	49	58	9	Severinghaus et al. (2001)
Dome C	-54.5	2.7	30	97	100	3	Landais et al. (2006)
WAIS Divide	-31	22	38	~67	76.5	9.5	Battle et al. (2011)
NEEM	-28.9	22	48	63	78	15	Buizert et al. (2012a)
NGRIP	-31.1	19	45	67.5	78	11.5	Kawamura et al. (2006)
Summit	-32	23	27	70	80.8	10.8	Witrant et al. (2012)

492 **Table 2. Comparison of standard deviation of density (σ_ρ) at critical density (ρ_{crit}). For data from all other**
493 **sites, except the Styx, refer to Hörhold et al. (2011).**
494

Campaign/Region	Core name	ρ_{crit} (kg m^{-3})	σ_ρ, ρ_{crit} (kg m^{-3})	T (°C)	A(cm ice yr^{-1})	σ_ρ, ρ_{crit} / A
Styx	Styx	821.68	19.33±1.87	-31.7	10	1.93±0.19
NGT	B16	819.27	12.26	-27	15.5	0.79
NGT	B18	820.81	12.81	-30	11.3	1.13
NGT	B21	820.81	12.91	-30	11.8	1.09
NGT	B26	820.85	13.23	-30.6	20	0.66
NGT	B29	821.32	10.50	-31.6	16.7	0.63
Berkner Island	B25	819.16	14.57	-27	15	0.97
DML	B31	827.00	10.27	-42	6.9	1.49
DML	B32	827.00	11.28	-42	6.7	1.68
DML	B36/37	827.50	8.12	-44.6	7.3	1.11
Pre-IPICS	B38	815.00	16.59	-18.1	136	0.12
Pre-IPICS	B39	814.91	17.11	-17.9	84	0.20
Pre-IPICS	DML95	815.51	13.42	-19.2	60	0.22
Pre-IPICS	DML97	816.07	10.03	-20.4	53	0.19
Dome C	EDC2	832.02	4.59	-53	2.7	1.70
WAIS Divide	WDC06A	820.81	10.35	-31	22	0.47

495
496